Inorg. Chem. **2003**, *42*, 7967−7977

Kinetics and Mechanistic Studies of Anticarcinogenic Bisperoxovanadium(V) Compounds: Ligand Substitution Reactions at Physiological pH and Relevance to DNA Interactions

Jung H. Hwang, Rhonda K. Larson, and Mahdi M. Abu-Omar*

Department of Chemistry and Biochemistry, University of California, Los Angeles, California 90095-1569

Received August 29, 2003

Bisperoxovanadium(V) compounds with bidentate ligands have shown tumor growth inhibition by cleaving DNA. The kinetics and mechanisms of ligand substitution reactions of two bisperoxovanadium(V) compounds $[VO(O_2)_2(bpy)]^-$ (bpVbpy) and $[VO(O_2)_2(phen)]^-$ (bpVphen) with entering ligands picolinic acid (pic) and dipicolinic acid (dipic) at physiological pH are reported, and its relevance to their DNA-cleavage activities are discussed. The products of the ligand substitution reactions with pic and dipic are the monoperoxo complexes $[VO(O_2)(pic)_2]^-$ and $[VO(O_2)(dipic)(H_2O)]^-$, respectively. ^{51}V NMR experiments indicate that bpVphen is substantially more inert in aqueous solution than bpVbpy. As a result, bpVbpy is more prone to ligand substitution and subsequent conversion to monoperoxo species. The rate of reaction for bpVbpy was faster than that of bpVphen by an order of magnitude, indicating that the ancillary ligand plays an important role in ligand substitution reactions. The ligand substitution reactions of bpVbpy feature first-order dependence on both $[pic]_T$ and $[dipic]_T$ whereas the substitution kinetics of bpVphen feature saturation behavior with dipic. The substitution reactions of both bpVbpy and bpVphen with pic showed first-order dependence on $[H^+]$ whereas no acid dependence was observed for the reactions with dipic. Hydrogen peroxide was determined to be a competitive inhibitor with respect to dipic. The ligand substitution reaction mechanisms and the rate laws consistent with these results are presented. The substitution reactions with pic and dipic proceed through different mechanisms; the substitution reactions with dipic proceed via solvolysis as the first step in the mechanisms whereas the reactions with pic bypass solvolysis to go through a mixed ligand monoperoxo vanadium intermediate.

Introduction

Vanadium is found naturally in soil and water as a trace metal. Vanadium compounds with oxidation states of III, IV, and V exist in the environment and in biological systems. The chemistry of the two latter oxidation states, in the form of vanadyl(IV) and vanadate(V), is particularly relevant to the biological action and the effects of vanadium in mammals.[1] Especially, vanadate has been shown to exert insulin-like effect,[2−6] and the oral administration of vanadate has been proven to reduce hyperglycemia in diabetic rats.[7−11] The mechanism of this mimetic action has been studied extensively.[12,13]

Peroxovanadium compounds[14] are also known to mimic insulin in vitro and in vivo via phosphotyrosine phosphatase inhibition.[15−21] Furthermore, these compounds have been

* Author to whom correspondence should be addressed. Present address: Department of Chemistry, Purdue University, 560 Oval Drive, West Lafayette, IN 47907. Fax: (765) 494-0239. E-mail: mabuomar@Purdue.edu.

(1) Crans, D. C.; Tracey, A. S. In *Vanadium Compounds: Chemistry, Biochemistry, and Therapeutic Applications*; Tracey, A. S., Crans, D. C., Eds.; American Chemical Society: Washington, D. C., 1998; Vol. 711, pp 2−29.
(2) Tolman, E. L.; Barris, E.; Burns, M.; Pansini, A.; Partridge, R. *Life Sci.* **1979**, *25*, 1159−1164.
(3) Dubyak, G. R.; Keinzeller, A. *J. Biol. Chem.* **1980**, *255*, 5306−5312.
(4) Shechter, Y.; Karlish, S. J. D. *Nature* **1980**, *284*, 556−558.
(5) Tamura, S.; Brown, T. A.; Whipple, J. H.; Fujita-Yamaguchi, Y.; Dubler, R. E.; Cheng, K.; Larner, J. *J. Biol. Chem.* **1984**, *259*, 6650−6658.
(6) Kadota, S.; Fantus, I. G.; Hersh, B.; Posner, B. I. *Biochem. Biophys. Res. Commun.* **1986**, *138*, 174−178.
(7) Heyliger, C. E.; Tahiliani, A. G.; McNeill, J. H. *Science* **1985**, *227*, 1474−1477.
(8) Meyerovitch, J.; Farfel, Z.; Sack, J.; Shechter, Y. *J. Biol. Chem.* **1987**, *262*, 6658−6662.
(9) Brichard, S. M.; Okitolonda, W.; Henquin, J. C. *Endocrinology* **1988**, *123*, 2048−2053.
(10) Gil, J.; Miralpeix, J.; Carreras, J.; Bartons, R. *J. Biol. Chem.* **1988**, *263*, 1868−1871.
(11) Blondel, O.; Bailbe, D.; Portha, B. *Diabetologia* **1989**, *32*, 185−190.

10.1021/ic0350180 CCC: $25.00
Published on Web 10/28/2003

Scheme 1

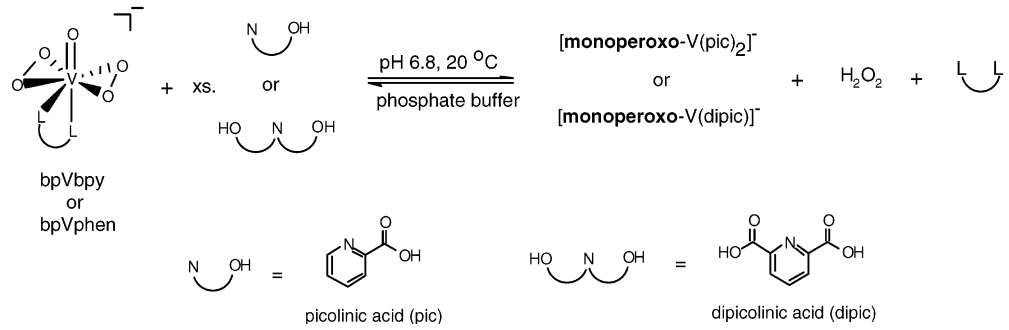

shown to inhibit cancerous tumor growth[22−25] and to induce DNA cleavage chemically and photochemically.[26−28] Recently, Kwong et al.[29] examined DNA-photocleavage activities of 15 peroxovanadium compounds by using a plasmid DNA relaxation assay.[30] Among the 15 compounds that were examined, $[VO(O_2)_2(phen)]^-$ (phen = 1,10-phenanthroline) showed the highest DNA-cleavage activity, that is, 99%. The authors proposed the possibility of singlet oxygen as the cleavage source. However, the mechanism of DNA cleavage by these peroxovanadium compounds has not been elucidated yet. Also, an interesting finding was that $[VO(O_2)_2(phen)]^-$ and $[VO(O_2)_2(bpy)]^-$ (bpy = 2,2′-bipyridine) showed a substantial difference in DNA-cleavage activities: 99% vs 50%, respectively. It is surprising that the subtle change in the ancillary ligand from phen to bpy resulted in a ∼50% decrease in the DNA-cleavage activity. The origin of this difference has not been explained. The above report by Kwong et al. prompted us to investigate the aqueous chemistry and the reaction kinetics of the bisperoxovanadium complexes, $[VO(O_2)_2(phen)]^-$ and $[VO(O_2)_2(bpy)]^-$, at physiological pH.

It has been previously reported that addition of ancillary ligand (e.g., phen) retards the DNA-cleavage activity of $[VO(O_2)_2(phen)]^-$.[28] Thus, dissociation of the ancillary ligand must be involved in the interaction between the bisperoxovanadium compounds and DNA. In other words, a ligand substitution reaction takes place. Kinetics and mechanisms of formation and decomposition of some peroxovanadium compounds have been reported in the literature. Also, reactions of peroxovanadates with amino acids and small peptides have been studied using ^{1}H NMR and ^{51}V NMR.[31−34] However, these studies were done exclusively with simple peroxovanadate[31−39] or in acidic pH.[38−41] The kinetics and mechanisms of ligand substitution reactions of bisperoxovanadium complexes with ancillary ligands (e.g., $[VO(O_2)_2(L-L)]^-$), which employ small organic molecules as entering ligands, at *neutral*, *physiological* pH have not been defined. Therefore, we investigated ligand substitution reactions of $[VO(O_2)_2(bpy)]^-$ and $[VO(O_2)_2(phen)]^-$ with picolinic acid and dipicolinic acid at physiological pH (Scheme 1). Herein, we report on the kinetics and mechanisms of these reactions and the relevance of the kinetics and mechanisms of ligand substitution to the DNA-cleavage activities of $[VO(O_2)_2(bpy)]^-$ and $[VO(O_2)_2(phen)]^-$.

Experimental Section

Materials. Ammonium vanadate (NH_4VO_3) was purchased from Matheson Co. Bpy, phen, picolinic acid, and 2,6-pyridinedicar-

(12) Shechter, Y.; Eldberg, G.; Shisheva, A.; Gefel, D.; Sekar, N.; Qian, S.; Bruck, R.; Gershonov, E.; Crans, D. C.; Goldwasser, Y.; Fridkin, M.; Li, J. In *Vanadium Compounds: Chemistry, Biochemistry, and Therapeutic Applications*; Tracey, A. S., Crans, D. C., Eds.; American Chemical Society: Washington, D.C., 1998; Vol. 711, pp 308−315 and references therein.
(13) Thompson, K. H.; McNeill, J. H.; Orvig, C. *Chem. Rev.* **1999**, *99*, 2561−2571 and references therein.
(14) Butler, A.; Clague, M. J.; Meister, G. E. *Chem. Rev.* **1994**, *94*, 625−638.
(15) Kadota, S.; Fantus, I. G.; Deragon, G.; Guyda, H. J.; Hersh, B.; Posner, B. I. *Biochem. Biophys. Res. Commun.* **1987**, *147*, 259−266.
(16) Posner, B. I.; Faure, R.; Burgess, J. W.; Bevan, A. P.; Lachance, D.; Zhang-Sun, G.; Fantus, I. G.; Ng, J. B.; Hall, D. A.; Lum, B. S.; Shaver, A. *J. Biol. Chem.* **1994**, *269*, 4596−4604.
(17) Shaver, A.; Ng, J. B.; Hall, D. A.; Posner, B. I. *Mol. Cell. Biochem.* **1995**, *153*, 5−15.
(18) Yale, J. F.; Vigeant, C.; Nardolillo, C.; Chu, Q.; Yu, Z.-Z.; Shaver, A.; Posner, B. I. *Mol. Cell. Biochem.* **1995**, *153*, 181−190.
(19) Band, C. J.; Posner, B. I.; Dumas, V.; Contreres, J. O. *Mol. Endocrinol.* **1997**, *11*, 1899−1910.
(20) Westergaard, N.; Brand, C. L.; Lewinsky, R. H.; Anderson, H. S.; Carr, R. D.; Burchell, A.; Lundgren, K. *Arch. Biochem. Biophys.* **1999**, *366*, 55−60.
(21) Brand, R. M.; Hamel, F. G. *Int. J. Pharm.* **1999**, *183*, 117−123.
(22) Djordjevic, C. In *Metal Ions in Biological Systems: Vanadium and Its Role in Life*; Sigel, H., Sigel, A., Eds.; Marcel Dekker: New York, 1995; Vol. 31, pp 595−616.
(23) Djordjevic, C.; Wampler, G. L. *J. Inorg. Biochem.* **1985**, *25*, 51−55.
(24) Hanauska, U.; Hanauska, A. R.; Marshall, M. H.; Muggia, V. A.; Von Hoff, D. D. *Int. J. Cell Cloning* **1987**, *5*, 170−178.
(25) Ban, J.; Maysinger, D.; Kovac, V.; Galetic, I.; Matulic, M.; Hadzija, M.; Uzarevic, B. *Life Sci.* **2000**, *68*, 165−175.
(26) Sakurai, H.; Nakai, M.; Mika, T.; Tsuchiya, K.; Takada, J.; Matsushita, R. *Biochem. Biophys. Res. Commun.* **1992**, *189*, 1090−1095.
(27) Hiort, C.; Goodisman, J.; Dabrowiak, J. C. *Mol. Cell. Biochem.* **1995**, *153*, 31−36.
(28) Hiort, C.; Goodisman, J.; Dabrowiak, J. C. *Biochemistry* **1996**, *35*, 12354−12362.
(29) Kwong, D. W. J.; Chan, O. Y.; Wong, R. N. S.; Musser, S. M.; Vaca, L.; Chan, S. I. *Inorg. Chem.* **1997**, *36*, 1276−1277.
(30) Brawn, K.; Fridovich, I. *Arch. Biochem. Biophys.* **1981**, *206*, 414−419.
(31) Tracey, A. S.; Jaswal, J. S. *J. Am. Chem. Soc.* **1992**, *114*, 3835−3840.
(32) Tracey, A. S.; Jaswal, J. S. *Inorg. Chem.* **1993**, *32*, 4235−4243.
(33) Jaswal, J. S.; Tracey, A. S. *J. Am. Chem. Soc.* **1993**, *115*, 5600−5607.
(34) Elvingson, K.; Crans, D. C.; Petterson, L. *J. Am. Chem. Soc.* **1997**, *119*, 7005−7012.
(35) Clague, M. J.; Butler, A. *J. Am. Chem. Soc.* **1995**, *117*, 3475−3484.
(36) Jaswal, J. S.; Tracey, A. S. *Inorg. Chem.* **1991**, *30*, 3718−3722.
(37) Bonchio, M.; Conte, V.; Di Furia, F.; Modena, G.; Moro, S.; Edwards, J. O. *Inorg. Chem.* **1994**, *33*, 1631−1637.
(38) Orhanovic, M.; Wilkins, R. G. *J. Am. Chem. Soc.* **1967**, *89*, 278−282.
(39) Conte, V.; Di Furia, F.; Moro, S. *J. Mol. Catal.* **1994**, *94*, 323−333.
(40) Wieghardt, K. *Inorg. Chem.* **1978**, *17*, 57−64.
(41) Quilitzsch, U.; Wieghardt, K. *Inorg. Chem.* **1979**, *18*, 869−871.

boxylic acid (dipicolinic acid) were purchased from Aldrich. H_2O_2 (30% w/v) was purchased from Fisher Scientific Co. Deuterium oxide (D_2O, 99.9%) was purchased from Cambridge Isotope Laboratories, Inc. Absolute ethanol was purchased from Gold Shield Chemical Co. All chemicals were of reagent grade or the highest purity available and were used without further purification. The complexes $NH_4[V(O)(O_2)_2(bpy)]\cdot 4H_2O$ (bpVbpy) and $NH_4[V(O)(O_2)_2(phen)]\cdot 2H_2O$ (bpVphen) were prepared as described in the literature.[42] The complexes were fully characterized by UV−vis, IR, and ^{51}V NMR.

Instrumentation. IR spectra were recorded on a JASCO FT/IR-420 infrared spectrometer on a 3M polyethylene card Type 91. UV−vis spectra were recorded on a Shimadzu UV-2501 PC spectrometer, equipped with a thermostated cell compartment. ^{51}V NMR spectra were collected on a Bruker ARX-500 MHz NMR, and $VOCl_3$ was used as an external reference. A 1:1 mixture of D_2O and 0.10 M, pH 6.8 sodium phosphate buffer ($[NaH_2PO_4]/[Na_2HPO_4]$) was used as the solvent for ^{51}V NMR experiments. Stopped-flow kinetics were collected on an Applied Photophysics SX.18MV stopped-flow spectrometer. pH measurements were performed on a Corning pH meter 430.

Kinetics. Unless otherwise noted, all kinetics measurements were carried out at 20 °C in 0.10 M, pH 6.8 sodium phosphate buffer ($[NaH_2PO_4]/[Na_2HPO_4]$), with excess NH_4Cl to maintain the ionic strength (μ = 1.00 M). The final products from the ligand substitution reactions were characterized by UV−vis and ^{51}V NMR.

In ligand substitution reactions, 0.90 mM bpVbpy or bpVphen was reacted with excess pic (10.0−60.0 mM) or dipic solution (2.5−35.0 mM). The changes in absorbance at 350 and 366 nm were monitored for bpVbpy and bpVphen, respectively. The reported rate constants were determined using the initial rates method.

The effect of light on the rates of ligand substitution was also examined using a 100-W mercury lamp ($\lambda_{irr} \sim 350$ nm). A UG-1 glass filter and a copper sulfate solution filter were used to cut off the visible (425−675 nm) and IR regions, respectively.

The effect of pH on the rates of ligand substitution was examined by conventional UV−vis and stopped-flow spectrometer. The pH ranges of 2−7 and 4.5−7 in 0.1 M sodium phosphate buffer were used for the reactions with pic and dipic, respectively. Due to the low solubility of dipic, a narrower pH range (4.5−7) was utilized. At pH below 4, dipic precipitates out of solution. The pH of each solution was adjusted by adding appropriate amounts of concentrated HCl or NaOH. For the reactions of bpVphen with pic below pH 3, in which the reactions are too fast to monitor by conventional UV−vis, stopped-flow was utilized.

Inhibition by H_2O_2 was investigated by UV−vis for ligand substitution reactions of bpVphen. Several entering ligand (dipic: 10 and 30 mM; pic: 50 mM) and H_2O_2 (10, 20, 30, 50, and 500 mM) concentrations were used.

The effect of H_2O_2 concentration on the monoperoxo products was probed by UV−vis and ^{51}V NMR. Solutions containing 0.9 mM bpVphen and excess dipic (10 and 30 mM) or pic (50 mM) were allowed to equilibrate overnight, prior to the addition of excess H_2O_2.

Results

General Features of Vanadium Peroxo Complexes and Their Ligand Substitution Reactions. The bisperoxovanadium complexes (bpVbpy and bpVphen) showed the expected IR stretches and UV−vis extinction coefficients (Table S1 and Figure S1, see Supporting Information).[42] The presence of two O−O stretches in the IR spectra is consistent with the assignment of two peroxo ligands on vanadium. In addition, each compound exhibited a single ^{51}V NMR peak around −748 ppm, which is in the expected range for bisperoxo complexes.[17,43] However, bpVbpy and bpVphen exhibit different stability in solution. For example, when bpVbpy is dissolved in a 1:1 mixture of D_2O and 0.10 M, pH 6.8 phosphate buffer, a peak at −697 ppm appears approximately after 6 h. This peak is due to $[V(O)(O_2)_2(H_2O)_2]^-$.[17,43] Thus, the bpy ligand on bpVbpy dissociates, producing the bisperoxo-aqua species. In contrast, the phen complex, bpVphen, is stable for more than 2 days in solution. Nevertheless, solutions of the vanadium peroxo complexes were freshly prepared before each experiment.

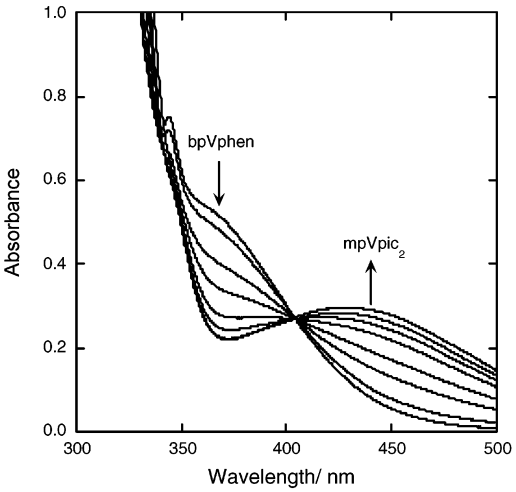

Figure 1. Absorption spectra of bpVphen (0.9 mM) in a 0.10 M, pH 6.8 sodium phosphate buffer, in the presence of increasing amount of pic (0−0.3 M).

In all kinetic experiments, the absorbance changes at 350 nm and at 366 nm were monitored for bpVbpy and for bpVphen, respectively, since absorption at these wavelengths exhibited maximum changes upon ligand substitution. A titration plot of bpVphen with pic is shown in Figure 1. The shoulder at 366 nm decreases while a broad band at 450 nm increases. The broad band at 450 nm represents the monoperoxo-picolinate ($mpVpic_2$) species.[40,41,44] The molar extinction coefficients for both complexes, at 350 nm for bpVbpy and 366 nm for bpVphen, were determined using Beer's Law plots: ϵ_{350nm}(bpVbpy) = 604 ± 2 M^{-1} cm^{-1} and ϵ_{366nm}(bpVphen) = 563 ± 2 M^{-1} cm^{-1}. The concentrations of the compounds in solutions were calculated using the above molar extinction coefficients. pic and dipic were chosen as the entering ligands for ligand substitution studies because their reactions with bpVbpy and bpVphen produced a clean, single-product species with no side products. When oxalate and citrate were used as entering ligands for the ligand substitution reactions with bpVbpy, the substitution reactions yielded multiple products and exhibited complex kinetics.

(42) Vuletic, N.; Djordjevic, C. *J. Chem. Soc., Dalton Trans.* **1973**, 1137−1141.

(43) Conte, V.; Di Furia, F.; Stefano, M. *Inorg. Chim. Acta* **1998**, *272*, 62−67.

(44) Djordjevic, C.; Vuletic, N.; Renslo, M. L.; Puryear, B. C.; Alimard, R. *Mol. Cell. Biochem.* **1995**, *153*, 25−29.

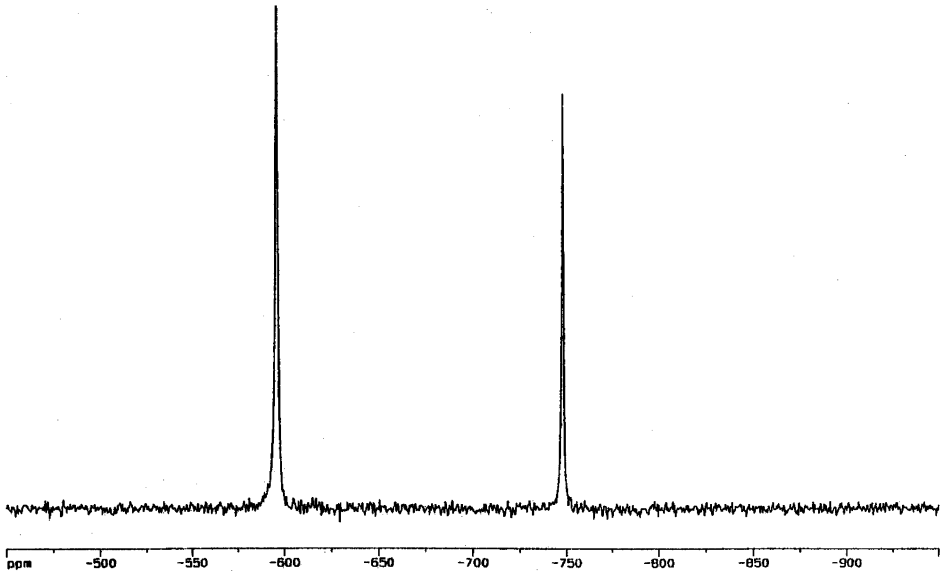

Figure 2. ^{51}V NMR spectrum of a mixture containing bpVbpy (0.9 mM) and dipic (30 mM) in a 1:1 mixture of D_2O and 0.10 M, pH 6.8 sodium phosphate buffer, taken 20 min after the beginning of the reaction.

For example, the reaction of bpVbpy with citrate gave six different peaks in the ^{51}V NMR spectrum. On the other hand, the reaction of bpVbpy with dipic features two distinctive peaks in the ^{51}V NMR spectrum, δ −748 for bpVbpy and δ −596 for $[V(O)(O_2)(dipic)(H_2O)]^-$, mpVdipic, without accumulation of intermediates (Figure 2).[17] Also, Figure 1 features a distinct isosbestic point at ∼405 nm, indicating that a single set of reactants gives a single set of products in constant proportions.[45]

Ligand Substitution Kinetics. The ligand substitution reactions of bpVbpy and bpVphen with pic and dipic yield the monoperoxo complexes (Scheme 1). The substitution reaction with dipic produces $[V(O)(O_2)(dipic)]^-$ (mpVdipic) whereas the reaction with pic produces $[V(O)(O_2)(pic)_2]^-$ ($mpVpic_2$). In the case of pic, the bpy or phen ligand and one of the two peroxo groups are replaced by two molecules of pic. The ^{51}V NMR spectrum of a reaction mixture containing bpVphen (0.9 mM) and pic (50 mM) in a 1:1 mixture of D_2O and 0.10 M, pH 6.8 sodium buffer, taken after completion of the ligand substitution reaction, shows a single peak at −632 ppm. This peak is assigned as $mpVpic_2$ whereas mpVpic with only one pic ligand on vanadium occurs at −600 ppm.[17,43,44,46]

The extent of the ligand substitution reactions depended on the concentrations of the entering ligands. As revealed by UV−vis, the final absorbance values at the end of substitution reactions varied with the entering ligand concentrations (data not shown). This result indicates that the ligand substitution reactions are reversible (i.e., in equilibrium).

As shown in Figure 3, the observed first-order rate constants ($k_{obs} = v_i/[bpV(L-L)]_i$, s^{-1}) of the ligand substitution reaction with bpVbpy and bpVphen reveal a linear, first-order dependence on $[pic]_T$. The most striking difference between pic and dipic is that the ligand substitution reaction

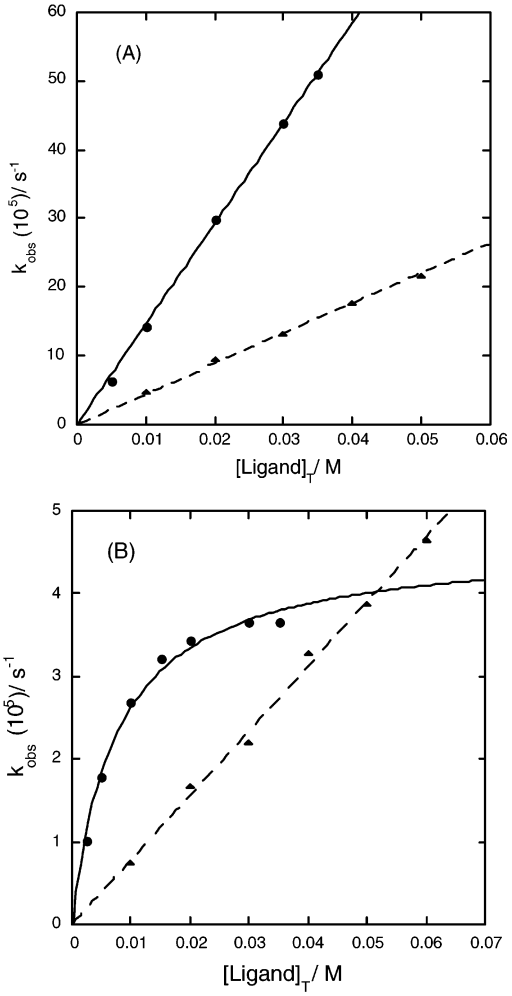

Figure 3. (A) Plot of k_{obs} vs $[ligand]_T$ with 0.9 mM bpVbpy: dipic (●, —) and pic (▲, − − −). (B) Plot of k_{obs} vs $[ligand]_T$ with 0.9 mM bpVphen: dipic (●, —) and pic (▲, − − −). Observed first-order rate constants (k_{obs}) are summarized in Table S2 in the Supporting Information.

of bpVphen with dipic shows saturation behavior at $[dipic]_T > 0.020$ M (Figure 3B), whereas pic shows a linear, first-

(45) Moore, J. W.; Pearson, R. G. *Kinetics and Mechanism*; 3rd ed.; Wiley-Interscience: New York, 1981; pp 49−50.

order dependence with both bpVbpy and bpVphen. Also, the rate at $[pic]_T > 0.050$ M *exceeds* the plateau value (saturation) of the observed rate (i.e., the maximum k_{obs}) for the reaction of bpVphen with dipic. These results indicate that the ligand substitution reactions with pic and dipic proceed through different mechanisms.

It is noteworthy that the substitution reaction rates for bpVbpy are an order of magnitude faster than those for bpVphen. Also, the reaction of bpVbpy with dipic does not feature saturation kinetics. Again, this result demonstrates the differences in substitution kinetics between bpVbpy and bpVphen.

The effect of light on the rate of ligand substitution for bpVphen is shown in Figure S2 in the Supporting Information. A reaction mixture containing bpVphen (0.9 mM) and pic (50 mM) was irradiated ($\lambda_{irr} \sim 350$ nm) for the entire duration of the substitution reaction. The presence of light enhances the rate of reaction 2-fold. The observed first-order rate constant for photochemical substitution is $(6.9 \pm 0.1) \times 10^{-5}$ s^{-1}, whereas the observed rate for the thermal reaction is $(3.88 \pm 0.02) \times 10^{-5}$ s^{-1}. The rate enhancement due to photolysis can be explained as a result of photochemical dissociation of a peroxo ligand.

pH Profile. The pH dependence of the ligand substitution reactions was determined. At the end of each reaction, the pH of the reaction solution was measured to verify that the pH remained constant throughout the reaction. Figure 4 shows the pH profiles for the reactions of bpVbpy and bpVphen (both 0.9 mM) with 50 mM pic, 10 mM dipic, and 30 mM dipic. For the reactions of bpVphen, the employed concentrations of dipic, that is, 10 and 30 mM, were chosen to represent the linear, first-order ligand dependence region and the ligand-saturated, zero-order dependence region, respectively (see Figure 3B). pic features a linear pH profile, characteristic of first-order dependence on $[H^+]$ over a pH range of 2−7. In contrast, the reactions of bpVphen with dipic (*both* 10 and 30 mM) exhibit no dependence on $[H^+]$ over the pH range of 4.5−7, Figure 4A. For the reactions of bpVbpy, pic features first-order dependence on $[H^+]$, Figure 4B. dipic, however, shows an intermediate slope (ca. -0.31 ± 0.03), indicating that the acid dependence is between zero- and first-order for the reaction of bpVbpy with dipic.

H_2O_2 Inhibition. Since ligand substitution reactions of bisperoxovanadium complexes yield monoperoxo−vanadium species, hydrogen peroxide is expected to inhibit the reaction. Indeed, when excess hydrogen peroxide ($[H_2O_2] = 500$ mM) is added to a reaction mixture containing 0.9 mM bpVphen and 50 mM pic, the ligand substitution reaction comes to a halt (data not shown). Representative time profiles for reactions of 0.9 mM bpVphen and 50 mM pic in the presence of various amounts of H_2O_2 (0, 20, and 50 mM) are shown in Figure S3 in the Supporting Information. The rate of the reaction containing 20 mM H_2O_2 is retarded noticeably by a factor of 5, and the reaction containing 50 mM H_2O_2 is completely inhibited.

(46) Conte, V.; Di Furia, F.; Moro, S. *J. Mol. Catal. A* **1997**, *117*, 139−149.

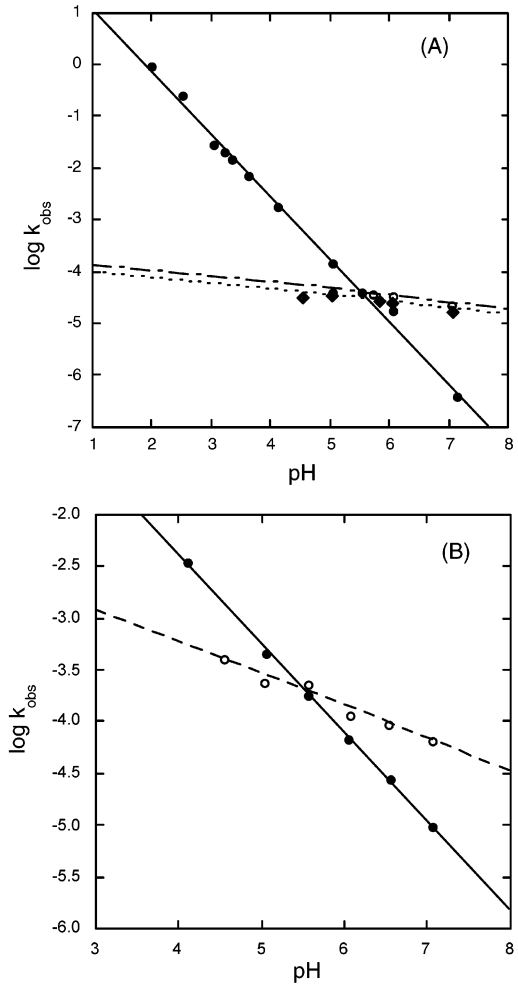

Figure 4. (A) Plot of log k_{obs} vs pH for the reactions of 0.9 mM bpVphen with 50 mM pic (●, —), 10 mM dipic (◆, - - -), and 30 mM dipic (○, - — -). (B) Plot of log(k_{obs}) vs pH for the reactions of 0.9 mM bpVbpy with 50 mM pic (●, —) and 30 mM dipic (○, — — —).

The hydrogen peroxide inhibition with dipic does not set in at the beginning of the reaction, as observed for pic. For instance, the ligand substitution reaction with 10 mM dipic proceeds undisturbed without any sign of inhibition for the initial 1000 s, even in the presence of 500 mM H_2O_2 (Figure 5A). Then, the ligand substitution reaction is terminated, and the bisperoxo species is regenerated, as evident from the subsequent increase in absorbance. When an equal amount (10 mM) of hydrogen peroxide and dipic is present, the ligand substitution reaction is finished after approximately 5000 s. Thus, in the presence of added H_2O_2, the reactions of bpVphen with 10 mM dipic shows no inhibition initially, but the extent of reaction is less; the equilibrium lies in favor of bpVphen rather than mpVdipic.

In the limit of zeroth order in $[dipic]_T$ (i.e., ≥30 mM, see Figure 3B), the ligand substitution reaction features very little inhibition even at 500 mM H_2O_2 (Figure 5B). The most striking feature of the hydrogen peroxide inhibition with dipic is that the extent of inhibition is dependent on the concentration of dipic. As illustrated by Figure 5A,B, the absorbance values at equilibrium depends on the concentration of dipic. For example, when 500 mM H_2O_2 is present, the final absorbance is ∼0.493 with 10 mM dipic and ∼0.435 with

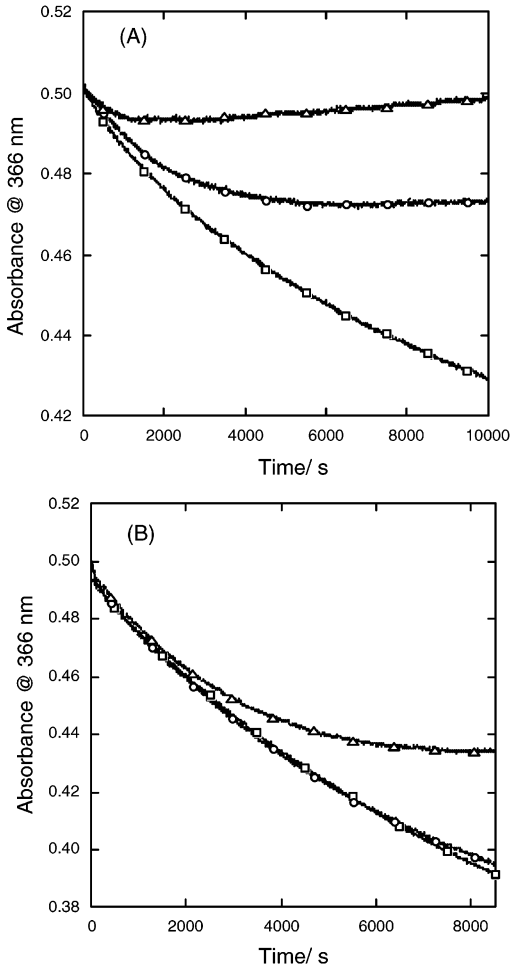

Figure 5. (A) Plot of absorbance vs time for reactions of 0.9 mM bpVphen with 10 mM dipic in the absence (□) and presence of 10 mM (○) and 500 mM (△) H_2O_2. (B) Plot of absorbance vs time for reactions of 0.9 mM bpVphen with 30 mM dipic in the absence (□) and presence of 30 mM (○) and 500 mM (△) H_2O_2.

30 mM dipic. In fact, in the presence of 30 mM H_2O_2 and 30 mM dipic, no inhibition effect upon the ligand substitution is observed, as apparent from the initial rates; $v_i = (3.28 \pm 0.02) \times 10^{-8}$ M s^{-1} in the absence of H_2O_2 versus $v_i = (3.24 \pm 0.02) \times 10^{-8}$ M s^{-1} in the presence of H_2O_2 (Figure 5B). Hence, hydrogen peroxide is a competitive inhibitor with respect to dipic.

When excess hydrogen peroxide (500 mM) is added after the substitution with dipic or pic is completed, the monoperoxo vanadium products (mpVpic$_2$ and mpVdipic) react with hydrogen peroxide through different routes. The identity of the generated bisperoxo complexes was examined by UV−vis and ^{51}V NMR. Our results indicate that mpVdipic in the presence of excess hydrogen peroxide reverts to the starting complex bpVphen, which is in line with our finding that the equilibrium of ligand substitution of bpVphen with dipic lies in favor of bpVphen rather than mpVdipic (vide infra). As evident by the absorption difference spectra shown in Figure 6, the UV−vis spectrum for the bisperoxo product from mpVdipic and excess H_2O_2 is identical to bpVphen. Furthermore, the addition of excess hydrogen peroxide to mpVdipic yields a chemical shift in the ^{51}V NMR that is consistent with bpVphen (δ −746.3). However, the bisperoxo

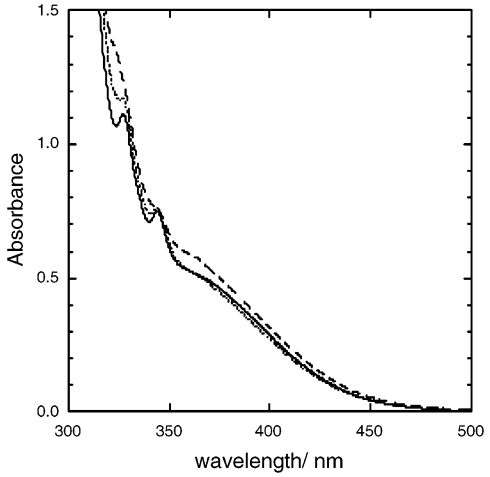

Figure 6. Absorption spectra of bpVphen (—), the bisperoxo species from mpVpic$_2$ (− − −), and the bisperoxo species from mpVdipic (- - -), after addition of 500 mM H_2O_2.

complex resulting from mpVpic$_2$ features a different absorption spectrum. The sharp peaks at ∼325 and 345 nm that are present in the bpVphen spectrum have disappeared. The bisperoxo complex from mpVpic$_2$ affords *consistently* a chemical shift that is 0.5 ppm more downfield (δ −745.8), Figure S4 (Supporting Information), than that observed for bpVphen. Since the known compound bpVpic ([V(O)(O$_2$)$_2$(pic)]$^{2-}$) occurs at −744 ppm,[17,43,46,47] we contend that the product from the addition of excess H_2O_2 to mpVpic$_2$ is a mixture of bpVphen and bpVpic. On the basis of these findings and the principles of microscopic reverse, ligand substitution reactions with pic and dipic proceed through different reaction intermediates.

Activation Parameters. The temperature dependence of the substitution reactions with pic and dipic was investigated over the temperature range of 10−40 °C at various ligand concentrations (Table 1). The data were used to construct linear Eyring plots (eq 1[48] and Figure S5 (Supporting Information)) from which the activation parameters $\Delta H^{\ddagger}$- and $\Delta S^{\ddagger}$ were determined. The values of rate constants along with activations parameters for ligand substitution reactions are summarized in Table 1. For the substitution reactions of bpVphen with 30 mM dipic, in the limit of zeroth order in [dipic]$_T$ (see Figure 3B), first-order rate constants were used to construct Eyring plots. In all other cases including the reactions of bpVphen with 10 mM dipic, the observed rate constants (k_{obs}) were normalized by the entering ligand concentrations since the substitution reactions are bimolecular and the rates depend on the entering ligand concentration. Thus, second-order rate constants (k, L mol^{-1} s^{-1}) were used in eq 1 for these cases.

$$\ln\left(\frac{k}{T}\right) = \ln\left(\frac{k_B}{h}\right) + \frac{\Delta S^{\ddagger}}{R} - \frac{\Delta H^{\ddagger}}{RT} \qquad (1)$$

As shown in Table 1, the values of $\Delta H^{\ddagger}$ determined for bpVphen are slightly higher than those for bpVbpy. More

(47) Shaver, A.; Ng, J. B.; Hall, D. A.; Lum, B. S.; Posner, B. I. *Inorg. Chem.* **1993**, *32*, 3109−3113.
(48) Espenson, J. H. *Chemical Kinetics and Reaction Mechanisms*, 2nd ed.; McGraw-Hill: New York, 1995; pp 156−164.

Table 1. Rate Constants and Activation Parameters for Ligand Substitution Reactions of bpVbpy and bpVphen[a]

		rate constants[b,c] (k), L mol^{-1} s^{-1}				
		bpVbpy		bpVphen		
T, K	L′ =	pic (50 mM)	dipic (30 mM)	pic (50 mM)	dipic (10 mM)[d]	dipic (30 mM)[e,f]
283		1.38×10^{-3}	5.62×10^{-3}	2.63×10^{-4}	6.78×10^{-4}	8.56×10^{-6}
293		4.35×10^{-3}	1.46×10^{-2}	7.76×10^{-4}	2.68×10^{-3}	3.65×10^{-5}
303		1.20×10^{-2}	5.28×10^{-2}	2.47×10^{-3}	8.29×10^{-3}	1.17×10^{-4}
313		3.11×10^{-2}	1.30×10^{-1}	7.71×10^{-3}	2.10×10^{-2}	3.33×10^{-4}
$\Delta H^{\ddagger}$, kJ mol^{-1}		73.9 ± 0.8	76.3 ± 3.9	80.6 ± 2.5	81.9 ± 3.4	87.2 ± 2.9
$\Delta S^{\ddagger}$, J mol^{-1} K^{-1}		-37.9 ± 2.6	-18.4 ± 13.0	-28.8 ± 8.3	-15.2 ± 11.5	-33.0 ± 9.8

[a] Experimental conditions: 0.9 mM bpV(L−L); L′ = entering ligand (pic or dipic); in 0.1 M pH 6.8 sodium phosphate buffer; ionic strength = 1.0 M. [b] All rate constants have error values less than 5%. [c] Bimolecular, second-order rate constants (except 30 mM dipic): $k = (v_i/[\text{bpV(L−L)}]_i)/[\text{L}']$. [d] In the limit of first-order dependence on $[\text{dipic}]_T$ (see Figure 3B). [e] In the limit of zeroth-order dependence on $[\text{dipic}]_T$. [f] Unimolecular, first-order rate constants: $k = v_i/[\text{bpV(L−L)}]_i$, s^{-1}.

Scheme 2

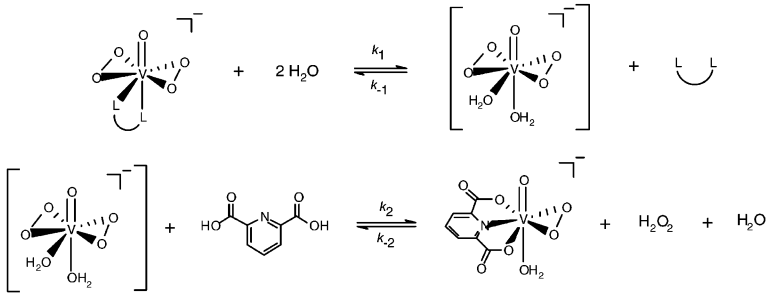

importantly, the values of $\Delta S^{\ddagger}$ for these reactions are not very negative, and $\Delta S^{\ddagger}$ for substitution reactions with dipic are somewhat less negative than those for the reactions with pic. For example, $\Delta S^{\ddagger}$ for the reaction of bpVbpy with pic is -38 J mol^{-1} K^{-1} whereas $\Delta S^{\ddagger}$ for the reaction with dipic is -18 J mol^{-1} K^{-1}. These activation parameters indicate that the reactions with pic and dipic proceed through different activation processes and thus different mechanisms. However, the small and negative values of $\Delta S^{\ddagger}$ in general indicate an I_a (Interchange, Associative) intimate mechanism for substitution on vanadium(V)−bisperoxo complexes.

Discussion

Substitution Reaction Mechanism: dipic. The bisperoxovanadium complexes, bpVbpy and bpVphen, react with pic and dipic to form monoperoxo species, mpVpic$_2$ and mpVdipic, respectively (Scheme 1). As stated above, our results indicate that the ligand substitution reactions of the bisperoxovanadium complexes with pic and dipic proceed through different mechanisms. The substitution reaction mechanisms must conform to the following: (1) the saturation behavior of bpVphen with dipic; (2) first-order dependence on pic; (3) first-order dependence and zeroth-order dependence on [H$^+$] with pic and dipic, respectively; and (4) competitive inhibition by H_2O_2 with respect to dipic for the reactions of bpVphen. The substitution reaction mechanism for the ligand substitution of bpV(L−L) with dipic is illustrated in Scheme 2.

As shown in Scheme 2, the mechanism consists of two reversible steps. The first step in the mechanism involves solvolysis and dissociation of the ancillary ligand (i.e., bpy and phen), thus forming bisperoxo-aqua complex ([bpV-$(H_2O)_2$]) as the reaction intermediate. It is possible that only one molecule of H_2O is coordinated to vanadium.[17,43,44] We do not have spectroscopic evidence to distinguish the number of H_2O molecules in the first coordination sphere of the intermediate species. Nonetheless, two molecules of H_2O are used in the solvolysis step to fulfill the coordination number of seven.[17,43] The second step of the mechanism involves association of the bisperoxo-aqua intermediate and fully protonated dipic to form mpVdipic, alongside the dissociation of H_2O_2 and one molecule of H_2O. Interestingly, fully protonated dipic is chosen as the reactive species in the second step of the mechanism since using deprotonated dipic as the reactive species results in a rate law that is not consistent with our results. The simplified, experimental rate law, derived according to the mechanism in Scheme 2, is given in eq 2, where $[\text{bpV(L−L)}]_t$ and $[\text{bpV(L−L)}]_e$ are the concentrations of bisperoxovanadium compound at time t and at equilibrium, respectively.[49] The full rate law and its derivation are given in the Supporting Information.

$$-\frac{\mathrm{d}[\text{bpV(L−L)}]}{\mathrm{d}t} = \left(\frac{k_1 k_2 [\text{dipic}]_T [\text{H}^+]^2}{k_2 [\text{dipic}]_T [\text{H}^+]^2 + k_{-2}[\text{H}_2\text{O}_2][\text{H}^+]^2}\right) ([\text{bpV(L−L)}]_t - [\text{bpV(L−L)}]_e) \quad (2.1)$$

$$-\frac{\mathrm{d}[\text{bpV(L−L)}]}{\mathrm{d}t} = \left(\frac{k_1 k_2 [\text{dipic}]_T}{k_2 [\text{dipic}]_T + k_{-2}[\text{H}_2\text{O}_2]}\right) ([\text{bpV(L−L)}]_t - [\text{bpV(L−L)}]_e) \quad (2.2)$$

The rate law in eq 2 is consistent with the experimental results. First, it explains the saturation behavior observed for bpVphen with dipic as well as the competitive inhibition of H_2O_2. In the limit of first-order dependence on $[\text{dipic}]_T$ (i.e., $[\text{dipic}]_T \leq 10$ mM), the observed rate constant becomes $k_{obs} = k_1 K_2 [\text{dipic}]_T / [\text{H}_2\text{O}_2]$, thus giving rise to first-order

dependence on $[dipic]_T$ and inhibition by H_2O_2. In the limit of zero-order dependence on $[dipic]_T$, the term $k_2[dipic]_T$ in the denominator dominates, and the observed rate constant reduces to k_1, which explains the saturation kinetics and the absence of H_2O_2 inhibition. The substitution reactions of bpVbpy, on the other hand, feature first-order dependence on $[dipic]_T$ over the wide concentration range investigated. As mentioned above, our ^{51}V NMR experiments revealed that bpVphen is substantially more stable in solution phase than bpVbpy; the dissociation of bpy from bpVbpy proceeds considerably faster than dissociation of phen from bpVphen. Hence, the solvolysis step for bpVbpy does not become rate determining, even at high dipic concentrations.

Furthermore, the rate law (eq 2.2) predicts no $[H^+]$ dependence, which agrees with experimental results over a broad range of pH (4.5−7), Figure 4A. In the case of bpVbpy, however, the pH profile gave a slope of −0.31, Figure 4B. The slope is substantially lower than −1, indicating that the acid dependence is not first-order. Therefore, the slope of −0.31 in the case of bpVbpy must rise from contributions of other terms in the denominator of the full rate law (see Supporting Information), such as $k_{-2}K_{a_1}^{dipic}[H_2O_2][H^+]$ and/or $k_{-1}K_{a_1}^{dipic}[L-L][H^+]$.

The activation parameters (Table 1) provide insight into the mechanism. In the limit of zero-order $[dipic]_T$, the reaction of bpVphen with dipic (30 mM) affords, albeit small, a negative value of $\Delta S^{\ddagger}$ (-33.0 J mol^{-1} K^{-1}). Hence, the solvolysis step (k_1), which is rate-determining in that limit, is associative in character. The $\Delta S^{\ddagger}$ values for the reaction of bpVbpy with dipic and the reaction of bpVphen and dipic (10 mM), in the limit of first-order dependence on $[dipic]_T$, are quite small and comparable: -18.4 and -15.2 J mol^{-1} K^{-1}, respectively (Table 1). In fact, within experimental precision these values are essentially zero. When the reactions are first-order in $[dipic]_T$, the observed rate constant reduces to $k_1K_2[dipic]_T/[H_2O_2]$ (eq 2.2). Thus, the observed rate constant, in the limit of first-order $[dipic]_T$, is a composite of elementary steps, and experimentally determined $\Delta S^{\ddagger}$ is the sum of $\Delta S_1^{\ddagger}$ and ΔS_2°.[48] The second step in the mechanism involves association of one molecule of dipic and dissociation of H_2O_2 and H_2O. Therefore, ΔS_2° for this equilibrium step is likely positive. As a result, the observed values of $\Delta S^{\ddagger}$ are *less* negative than those for the reactions of bpVphen with 30 mM dipic.

To examine the validity of the above mechanism for the substitution reactions with dipic, the kinetic simulation program HopKINSIM[50] was used to simulate time profiles. The mechanism shown in Scheme 2 was used in the simulation, which was contrasted to experimental data. Figure 7 displays experimental data alongside simulated time profiles. The value of k_1 was fixed to 4.0×10^{-5} s^{-1}, which is close to the saturation value from the least-squares fit in Figure 3B, since this value provided a simulated time profile that matches experimental data. All other rate constants were predicted values that provided best-fit. The initial rates of simulated kinetic traces were sensitive to k_1, whereas k_{-1}, k_2, and k_{-2} only affected the final absorbances (A_∞) and the curvatures of the traces.

For the substitution reaction of bpVphen with dipic, k_1 value of 4.0×10^{-5} s^{-1} provided a simulated kinetic trace that is in excellent agreement with the experimental time profile (Figure 7A). On the other hand, a k_1 value of 7.0×10^{-4} s^{-1} for the reaction of bpVbpy, approximately an order of magnitude larger than that of bpVphen, proved to yield a kinetic trace that matches experimental data (Figure 7B).

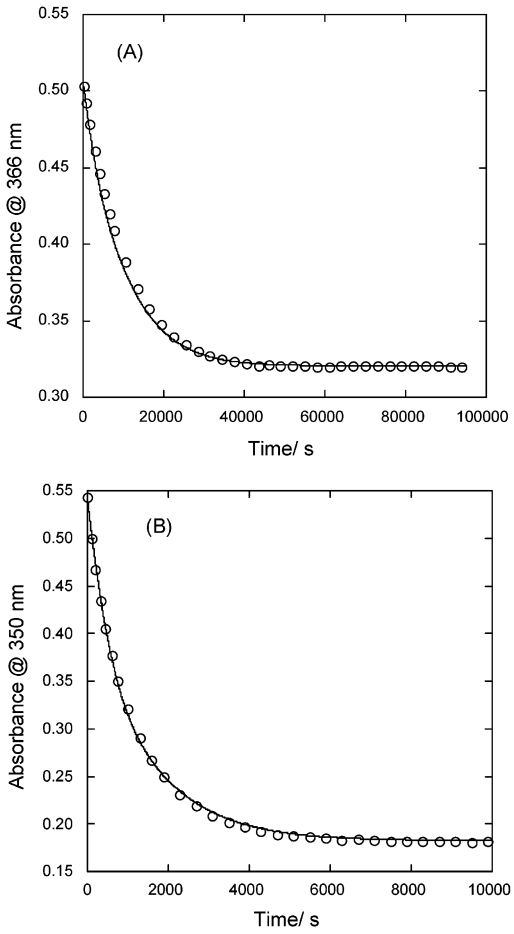

Figure 7. (A) Comparison of experimental data (○) and simulated kinetic trace (—) for the substitution reaction of bpVphen with dipic. Experimental conditions: $[bpVphen]_i = 0.90$ mM, $[dipic]_T = 30$ mM in 0.10 M, pH 6.8 sodium phosphate buffer at 20 °C. Simulation conditions: $[bpVphen]_0 = 0.90$ mM, $[dipic]_0 = 30$ mM, $k_1 = 4.0 \times 10^{-5}$ s^{-1}, $k_{-1} = 0.85$ M^{-1} s^{-1}, $k_2 = 6.5 \times 10^{-3}$ M^{-1} s^{-1}, $k_{-2} = 0.25$ M^{-1} s^{-1}. (B) Comparison of experimental data (○) and simulated kinetic trace (—) for the substitution reaction of bpVbpy with dipic. Experimental conditions: $[bpVbpy]_i = 0.90$ mM, $[dipic]_T = 30$ mM in 0.10 M, pH 6.8 sodium phosphate buffer at 20 °C. Simulation conditions: $[bpVbpy]_0 = 0.90$ mM, $[dipic]_0 = 30$ mM, $k_1 = 7.0 \times 10^{-4}$ s^{-1}, $k_{-1} = 1.6$ M^{-1} s^{-1}, $k_2 = 2.0 \times 10^{-2}$ M^{-1} s^{-1}, $k_{-2} = 0.8$ M^{-1} s^{-1}.

(49) Experimentally important terms from the full rate law, which match our experimental results, are included in the simplified, experimental rate law. Note that the inhibition term by ancillary ligands (i.e., bpy and phen) is not included in eq 2. Due to the low solubility of phen in aqueous solvents, inhibition effect of phen on the substitution reactions was not investigated. Since the ancillary ligand dissociates in the mechanism, the term involving inhibition by ancillary ligands could very well be a contributor in the denominator of the simplified rate law ($k_{-1}[L-L][H^+]^2$, see Supporting Information). However, this inhibition term is omitted from the simplified, experimental rate law for clarity of discussion.

(50) The Macintosh version of KINSIM. See Barshop, B. A.; Wrenn, R. F.; Frieden, C. *Anal. Biochem.* **1983**, *130*, 134−145.

Scheme 3

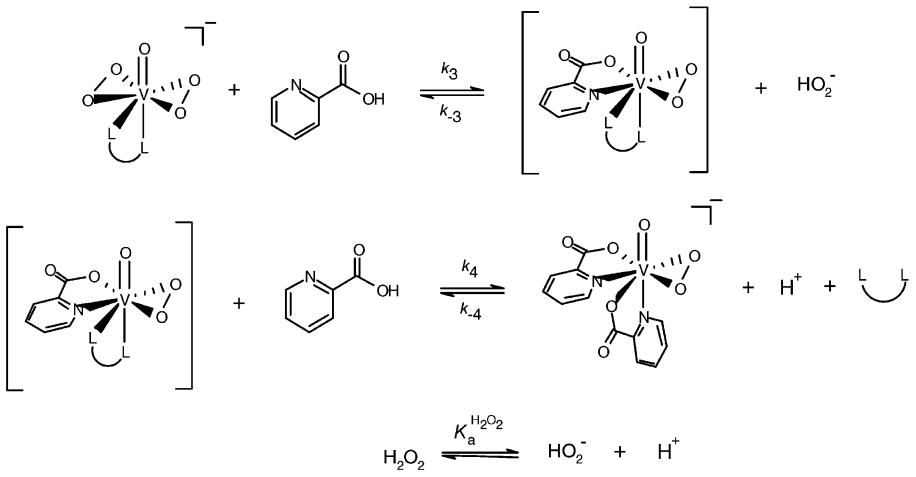

This, indeed, confirms solvolysis (k_1) as the rate-determining step.

Furthermore, according to the mechanism shown in Scheme 2, both bpVphen and bpVbpy give rise to the same reaction intermediate, namely, $[V(O)(O_2)_2(H_2O)_2]^-$. In other words, the values of k_2 and k_{-2} should be the same for both bpVphen and bpVbpy. Interestingly, for the best fits the actual predicted values of k_2 and k_{-2} for bpVbpy are slightly higher than those for bpVphen by a factor of 3. This discrepancy is rationalized by the fact that the reactions of bpVbpy with dipic are not as "clean-cut" as the reactions of bpVphen. For example, the difference in the pH dependence between bpVphen and bpVbpy (Figure 4) is a good point in case that illustrates contributions from other terms in the full rate law for bpVbpy. Nevertheless, the same $K_2(= k_2/k_{-2})$ of 0.025 is obtained for both bpVbpy and bpVphen. This again substantiates the hypothesis that the mechanism of substitution for bpVbpy and bpVphen with dipic is the same.

Substitution Reaction Mechanism: pic. The ligand substitution reactions of bpV(L−L) with pic must proceed through a different mechanism than the one described above for dipic since the observed rate constants at high $[pic]_T$ concentrations (i.e., >50 mM) exceed the plateau (saturation) value of the reactions with dipic. The reaction mechanism for ligand substitution on bpV(L−L) with pic is illustrated in Scheme 3. The simplified, experimental rate law for the mechanism is given in eq 3, where K_a^{pic} and $K_a^{H_2O_2}$ are the acid dissociation constants for pic and H_2O_2, respectively.[49] The full rate law and its derivation are included in the Supporting Information.

$$-\frac{d[bpV(L-L)]}{dt} = \left(\frac{k_3k_4[pic]_T^2[H^+]^3}{k_4K_a^{pic}[pic]_T[H^+]^2 + k_{-3}K_a^{H_2O_2}[H_2O_2][H^+]^2}\right)([bpV(L-L)]_t - [bpV(L-L)]_e) \quad (3.1)$$

$$-\frac{d[bpV(L-L)]}{dt} = \left(\frac{k_3k_4[pic]_T^2[H^+]}{k_4K_a^{pic}[pic]_T + k_{-3}K_a^{H_2O_2}[H_2O_2]}\right)([bpV(L-L)]_t - [bpV(L-L)]_e) \quad (3.2)$$

As shown in the mechanism, the first step of the ligand substitution reaction with pic is the association of protonated pic molecule and formation of $[VO(O_2)(pic)(L-L)]$ as an intermediate; the mechanism does not involve solvolysis. This may be attributed to the smaller size of pic compared to that of dipic. Thus, pic bypasses the solvolysis step. In the second step of the mechanism, a second molecule of protonated pic reacts with the mixed ligand intermediate to form the product $mpVpic_2$. In this mechanism, HO_2^- dissociates in the first step, whereas H_2O_2 is generated in the second step of the mechanism for dipic. HO_2^-, then, rapidly equilibrates with H^+ to form H_2O_2. Again, protonated pic is used as the reactive form since using deprotonated pic as the reactive species results in a rate law that is inconsistent with experimental results. The simplified, experimental rate law (eq 3) contains a $[pic]_T^2$ term in the numerator. Since our kinetics feature first-order dependence on $[pic]_T$ for both bpVbpy and bpVphen (Figure 3), $k_4K_a^{pic}[pic]_T \gg k_{-3}K_a^{H_2O_2}[H_2O_2]$. Hence, under the employed experimental conditions, and in the absence of excess hydrogen peroxide, the observed rate constant is (k_3/K_a^{pic})-$[pic]_T[H^+]$, which explains the first-order dependence on $[pic]_T$ and $[H^+]$. The first step (k_3) is rate-determining and the second step is fast. It is worth noting that having the solvated bisperoxo adduct, $V(O)(\eta^2\text{-}O_2)_2(OH_2)_2^-$, available for substitution with dipic would dictate that this same intermediate should in principle undergo substitution with pic; the intimate molecular reasons as to why the solvolysis intermediate does not react with pic is an intriguing observation and mystery to say the least.

Furthermore, the mechanism is consistent with H_2O_2 inhibition (Figure S3, see Supporting Information), which is more pronounced and different than that observed for dipic (Figure 5). In the mechanism for pic (Scheme 3), hydrogen peroxide dissociates in the rate-determining step (k_3). Contrarily, H_2O_2 dissociates in the second step of the mechanism for dipic (Scheme 2), which is not rate-determining. Therefore, H_2O_2 inhibits directly the rate of substitution with pic but only affects the equilibrium distribution in the case of dipic.

The values of $\Delta S^{\ddagger}$ for the reactions with pic are small and negative, which is characteristic of an I_a mechanism (Table

1). The rate-determining step for the reaction with pic is k_3, which involves association of pic. Therefore, both bpVbpy and bpVphen undergo substitution via an associative mechanism, whether the rate-determining step is solvolysis (in the case of dipic) or entry of the entering ligand (in the case of pic).

The kinetics of the substitution reactions investigated here are markedly different from other systems reported in the literature. Quilitzsch and Wieghardt have investigated the decomposition of several bisperoxovanadium complexes containing bidentate organic ligands to monoperoxovanadium complexes in perchloric acid media at low pH.[41] The proposed mechanism involves a rapid acid-catalyzed protonation of one of the peroxo moieties to form a coordinated, monodentate hydroperoxo ligand, V−O−OH, and the rate-determining step is protonation of the hydroperoxo ligand and dissociation of H_2O_2 to form a monoperoxo species, which subsequently binds water. Observed pseudo-first-order rate constants, k_{obs}, were determined to have the following forms:

$$k_{obs} = \frac{[H^+]}{a + b[H_2O_2]} \quad \text{or} \quad k_{obs} = c[H^+]$$

Our observed rate constant for the substitution reaction with pic (eq 3.2) is similar to the above form, which features an acid-dependent term. However, in the case of dipic, the observed rate constant features no pH dependence. Our proposed mechanisms (Schemes 2 and 3) for the substitution reactions of bpVbpy and bpVphen with pic and dipic at neutral pH do not involve protonation of a peroxo ligand. The similarity in the observed rate constant for the reaction with pic to that of Quilitzsch and Wieghardt must rise from the involvement of HO_2^- as the leaving group in the rate-determining step (Scheme 3). In the case of dipic, the rate-determining step is solvolysis (Scheme 2), in which acid has no involvement. Hence, this implies that, at neutral pH, protonation of a peroxo ligand becomes unimportant and solvolysis dominates the kinetics of ligand substitution reactions.

The formation of mpVdipic ($[VO(O_2)(dipic)(H_2O)]^-$) from the reaction of dioxodipicolinato vanadium ($[V(O)_2(dipic)]^-$) and hydrogen peroxide has also been investigated in acidic media.[40] From the kinetic data, the dioxodipicolinato complex was determined to be trimeric in solution. Hence, addition of H_2O_2 or HO_2^- (depending on the pH) to the trimer was proposed to occur via an associative pathway, followed by a subsequent breakdown (bridge cleavage) of the trimer. The resulting monomeric fragments were proposed to react with hydrogen peroxide to form two different bisperoxo complexes that contain two units of monodentate hydroperoxo ligands, V−O−OH. The bisperoxo complexes are then transformed to the final product, $[VO(O_2)(dipic)(H_2O)]^-$, via acid-catalyzed dissociation of H_2O_2 and formation of η^2-peroxo. Interestingly, Tanaka et al. investigated the same reaction of formation of mpVdipic from dioxodipicolinatovanadium(V) with hydrogen peroxide in acidic media and arrived at a different, complex rate law that included acid-dependent, acid-independent, and inverse acid terms.[51] Unlike the results reported by Wieghardt, the kinetics were consistent with a monomeric structure for the starting dioxodipicolinato complex $[V(O)_2(dipic)(H_2O)]^-$. Also, hydrolysis of the starting dioxodipicolinato complex to form the corresponding hydroxo complex, $[V(O)_2(dipic)(OH)]^{2-}$, was claimed to play a significant role in the reaction mechanism, in which both protonated aqua complex $[V(O)_2(dipic)(H_2O)]^-$ and unprotonated, hydroxo complex $[V(O)_2(dipic)(OH)]^{2-}$ react with H_2O_2 to form the final monoperoxo product. However, under the experimental conditions employed in our studies (pH 6.8), vanadium complexes containing hydroperoxo (V−O−OH) and hydroxo (V−OH) ligands were not observed by UV−vis or ^{51}V NMR.

Relevance of Substitution Reaction Kinetics and Mechanisms to DNA-Cleavage Activities. We have demonstrated herein that the reaction kinetics of bpVbpy and bpVphen at physiological pH are markedly different. The substitution reactions of bpVbpy feature first-order dependence on both $[pic]_T$ and $[dipic]_T$ whereas the kinetics of substitution for bpVphen feature saturation behavior with dipic, Figure 3. Also, the substitution reactions of bpVbpy proceed approximately 10 times faster than the analogous reactions of bpVphen. For the substitution reaction with dipic (Scheme 2), the first step of the reaction mechanism involves solvolysis and dissociation of the ancillary ligand. BpVphen is substantially more stable in solution than bpVbpy, and the bpy ligand is more prone to substitution than phen.

The difference in stabilities and reactivities of bpVbpy and bpVphen in solution can be correlated to the difference in their DNA-cleavage activities. Among the investigated bisperoxovanadium compounds, Kwong et al. found bisperoxo-aqua, $[VO(O_2)_2(H_2O)_2]^-$, to exhibit very low DNA-cleavage activity (i.e., 9%).[29] This indicates that the ancillary ligand plays an important role in DNA cleavage. Furthermore, monoperoxovanadium compounds displayed much lower efficiencies in DNA cleavage (3.5−30%). Our results reveal that bpVbpy is more prone to dissociation and substitution of the bpy ligand (thus, conversion to monoperoxo species) than bpVphen. Hence, it can be generalized that the higher DNA-cleavage activity exhibited by bpVphen compared to bpVbpy results from the higher kinetic robustness of bpVphen in solution and that the ancillary ligand must stay intact long enough to attain efficient DNA-cleavage activity.

Conclusions

We have reported herein the kinetics of ligand substitution reactions of bpVbpy and bpVphen with pic and dipic at physiological pH. As mentioned in the Introduction, previous kinetics studies of peroxovanadium compounds reported in the literature were performed with simple peroxovanadate or in acidic pH.[31−41] Most of those studies investigated the formation of simple peroxovanadate from orthovanadate and acid-catalyzed decomposition of peroxovanadate at low pH.

(51) Funahashi, S.; Haraguchi, K.; Tanaka, M. *Inorg. Chem.* **1977**, *16*, 1349−1353.

Table 2. Summary of Rate and Equilibrium Constants[a]

	entering ligand			
	dipic			pic
complex	k_1/s^{-1}	K_2	k_1K_2/s^{-1}	$k_3/M^{-1}\ s^{-1}$
bpVphen	$(4.6 \pm 0.2) \times 10^{-5}$	$(2.6 \pm 0.3) \times 10^{-2}$	$(1.2 \pm 0.2) \times 10^{-6}$	$(2.8 \pm 0.1) \times 10^{-2}$
bpVbpy[b]			$\sim 2.9 \times 10^{-6}$	$(1.6 \pm 0.1) \times 10^{-1}$

[a] pH 6.8 at 20 °C. [b] k_1K_2 is an estimate value since bpVbpy substitution with dipic shows some dependence on pH.

To our knowledge, the current system reported herein is the first example of kinetics and mechanisms of ligand substitution reactions involving bisperoxovanadium compounds with ancillary ligands and small organic molecules (i.e., pic and dipic) as entering ligands at physiological pH. Our kinetic results have revealed that bpVbpy and bpVphen display different stabilities in solution phase, bpVphen being substantially more stable, and the dissociation of the bpy ligand occurs more readily than phen. As a result, bpVbpy is more prone to ligand substitution reactions and, thus, conversion to monoperoxo species. The kinetics of substitution reaction of bpVphen feature saturation behavior with dipic whereas the substitution reactions of bpVbpy feature first-order dependence on both $[pic]_T$ and $[dipic]_T$. The rate and equilibrium constants for bpVbpy and bpVphen are summarized in Table 2.

Furthermore, the ligand substitution reaction mechanisms have been elucidated. The substitution reactions with dipic proceed through a solvolysis step whereas the substitution reactions with pic bypass solvolysis. Reports of ligand substitution reactions involving non-square-planar transition metal compounds in which the reaction proceeds through different mechanisms depending on the entering ligands are scarcely found in the literature. The only relevant example is the ligand substitution reaction of niobium(V) and tantalum(V) halides reported by Merbach and co-workers, in which the substitution reaction $MX_5L + L^* \leftrightarrows MX_5L^* + L$ ($M = Nb, Ta$; $X = Cl, Br$) proceeds via a dissociative mechanism when $L = Me_2O$ and via an associative mechanism when $L = Me_2S$, Me_2Se, Me_2Te.[52,53] The authors attributed this "mechanism crossover" mainly to the steric effects exerted by the entering ligands, which also applies to our current system. Interestingly, the transition metals employed in the reaction are niobium and tantalum, which are in Group VB as vanadium. Also, the metal centers are in the same oxidation state (+5) as bpVbpy and bpVphen.

As mentioned above, the stabilities and ligand substitution kinetics of bpVbpy and bpVphen are markedly different, and this difference can be correlated to the difference in their DNA-cleavage activities. We contend that the higher DNA-cleavage activity of bpVphen arises from its higher kinetic inertness in solution and that the ancillary ligand must stay intact for efficient DNA-cleavage activity. In conclusion, the current work demonstrates the unique kinetic behavior exhibited by bpVbpy and bpVphen at physiological pH and the dependence of their ligand substitution mechanisms on the identity of the entering ligand. The sterically less demanding pic ligand bypasses the solvolysis intermediate and enters the coordination sphere of bpV(phen/bpy) directly. Further investigations of bisperoxovanadium compounds will allow us to better understand their interaction with DNA and to fully elucidate their mechanism of DNA cleavage. Efforts along these lines are currently undergoing in our laboratory.

Acknowledgment. We wish to thank the NSF (CHE-9874857) and the Beckman Foundation (BYI to MMA) for financial support.

Supporting Information Available: Spectroscopic characterizations of peroxovanadium complexes, time profiles of substitution reactions, tables of observed rate constants, Eyring plots, and derivation of the rate laws. This material is available free of charge via the Internet at http://pubs.acs.org.

IC0350180

(52) Good, R.; Merbach, A. E. *Inorg. Chem.* **1975**, *14*, 1030−1034.
(53) Vanni, H.; Merbach, A. E. *Inorg. Chem.* **1979**, *18*, 2758−2762.